VNU Journal of Science: Mathematics – Physics, Vol. 31, No. 4 (2015) 49-55

Effects of Crystallinity and Particle Size on Photocatalytic Performance of $ZrTiO_4$ Nanostructured Powders

Le Thi Mai Oanh[1,2,*], Dang Thu Ha[2], Man Minh Hue[2], Lam Thi Hang[2,5], Dao Viet Thang[2,3], Nguyen Manh Hung[2,3], Doan Thuy Phuong[2,4], Nguyen Van Minh[1,2]

[1]*Physics Department, Hanoi National University of Education*
[2]*Nano Center of Science and Technology, Hanoi National University of Education*
[3] *Hanoi University of Mining and Geology*
[4]*University of Transport and Communications*
[5]*Hanoi University of Natural Resources and Environment*

Received 06 July 2015
Revised 15 September 2015; Accepted 12 November 2015

Abstract: The crystallinity, surface morphology, optical property and photocatalytic performance of $ZrTiO_4$ nanostructured powders synthesized by sol-gel method at various calcining temperatures were investigated by XRD, FE-SEM, and absorption measurements, respectively. XRD analysis showed that $ZrTiO_4$ began crystallizing at about 600 °C. The crystallinity increased with increasing calcining temperature. According to FE-SEM images, amorphous particles of nearly 10 nm in size with relatively sphere morphology were formed after a heat treatment of the $ZrTiO_4$ gel at 450 °C for 3 hours. The crystalline particle size increased gradually to 20, 50, and 100 nm when the calcining temperature increased to 800, 900, and 1000 °C, respectively. The UV-Vis absorption spectra indicated a slight broadening of optical band gap with increasing calcining temperature. Photodegradation performance of Rhodamine B (RhB) in aqueous solution via $ZrTiO_4$ nanopowders which occurred under the illumination of a Xenon lamp have showed that the $ZrTiO_4$ sample treated at 800 °C exhibited the largest efficiency of the photocatalytic performance.

Keywords: Nanopowder, photocatalytic, RhB, crystalline, amorphous.

1. Introduction

Zirconium titanate $ZrTiO_4$ recently attracted a huge consideration of researchers because it exhibits promising characteristics for many applications such as optics, photocatalysis, ceramic pigment and biomedicine [1-4]. With a high resistivity, a large dielectric constant, and an excellent thermal stability, $ZrTiO_4$ is particularly suitable for producing large storage capacitors and dielectric

*Corresponding author. Tel.: 84-985190882
Email: lemaioanh@gmail.com

resonators in telecommunication system. Many studies have shown that ZrO_2/TiO_2 binary oxides exhibited a high photocatalytic activity due to its high surface area and acidity (i.e. large surface hydroxyl groups) and also due to the large number of defects resulting from the substitution of zirconium into the TiO_2 lattice [5]. In addition, $ZrTiO_4$ also exhibited many advantages for a ceramic pigment base on its high melting point (T_m~1840 ºC), very high refractive index (n_x=2.33, n_y=2.38, n_z=2.41) and especially the existence of a distorted octahedral site which easily results in the intense chromatic effects [6, 7]. However, these applications demand high quality materials with high purity and homogeneity.

Sol-gel method is now well-known as a promising approach to synthesize homogenous $ZrTiO_4$ ceramic powders [8-10]. In this method, the crystallization temperature is much lower than that of the traditional route, such as melting and solid state reaction [11]. Additionally, the crystalline particle size could be easily controlled through calcining temperature and heat-treatment conditions to obtain the highest specific surface area of the samples.

In this work, an aqueous sol-gel method, as an environmentally friendly processing, was used to produce zirconium titanate nanopowders. The crystalline formation process was investigated by XRD method. Crystalline particle size and surface morphology were characterized by FE-SEM measurements. The absorption property and the photocatalytic performance of $ZrTiO_4$ nanopowders were characterized by UV-Vis spectra measurements.

2. Experimental

$ZrTiO_4$ nanopowders were synthesized by sol-gel process using titanium tetraisopropoxide TTIP ($Ti[OCH(CH_3)_2]_4$ Aldrich 97%) and zirconium (IV) oxychloride octahydrate ($ZrOCl_2 \cdot 8H_2O$ Aldrich 99%) as starting materials. Firstly, TTIP was gradually added to a solution containing deionized water and citric acid and magnetically stirred for 2 hours to get a transparent solution. An aqueous solution of zirconium (IV) oxychloride octahydrate was added dropwise into above Ti^{4+}-containing solution under magnetic stirring condition. Subsequently, ethylene glycol was used as a surface activation with the mole ratio between citric acid and ethylene glycol is about 6:4. The achieved solution was then continuously magnetic stirred at 90 ºC for about 2 hours to release water until a wet-gel was obtained. This gel was dried in 5 hours using a 150 °C oven to get a dry-gel. The final nanopowder products can be achieved by calcining the dry-gel at different temperatures from 350 to 1200 ºC for 3 hours.

Photocatalytic performance of the prepared $ZrTiO_4$ nanopowders was evaluated by the degradation of RhB. Photocatalytic processes were conducted in a glass cup (diameter is 6.5 cm) containing 100 ml of 10 ppm RhB solution under the illumination of a 300 W Xenon lamp. The illumination distance from the Xenon lamp to the solution surface is 8 cm. The absorbance of the RhB solution was investigated on a Jasco V670 UV-Vis spectrophotometer.

XRD patterns of $ZrTiO_4$ nanoparticles were recorded by a diffractometer (D8 Advance, Bruker) with Cu-Kα radiation. In order to determine the surface morphology by scanning electron microscopes FE-SEM, a Hitachi microscope (model S-4800) was used. The UV-Vis absorption spectra of the samples were recorded using Jasco V670 UV-Vis spectrophotometer.

Table 1. The abbreviation of $ZrTiO_4$ samples with different calcining temperatures.

Calcining temperature	350 °C	450 °C	500 °C	600 °C	700 °C	800 °C	1000 °C	1200 °C
Abbreviation	ZT350	ZT450	ZT500	ZT600	ZT700	ZT800	ZT1000	ZT1200

3. Results and discussion

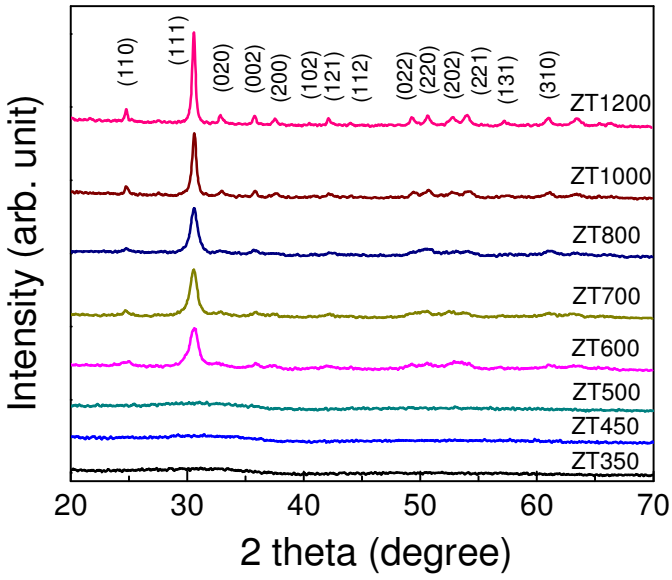

Figure 1. XRD patterns of $ZrTiO_4$ powders heat treated at different temperatures of 350, 450, 500, 600, 700, 800, 1000, and 1200 °C.

Fig. 1 shows XRD patterns of $ZrTiO_4$ nanopowders calcined at temperatures ranging from 350 to 1200 °C. From XRD it is obvious that $ZrTiO_4$ still existed in amorphous phase under the calcining temperature below 500 °C with the existence of broad halos pattern at about 2θ angle of 30°. The appearance of some XRD peaks in ZT600 pattern at 2θ angle of 24.8, 30.6, 32.5, 35.8, 37.3, 42.1, 44.0, 49.2, 50.5, 51.2, 56.8, and 61.1° indicates that $ZrTiO_4$ powder began crystallizing at the calcining temperature of about 600 °C. The increase of XRD peak intensities with the increase of the calcining temperature infers the better crystallization of $ZrTiO_4$ samples. The XRD pattern of ZT1200 sample corresponds to a best crystallization $ZrTiO_4$ phase showing the lattice parameters a = 4.797 Å, b = 5.449 Å, and c = 5.020 Å. These parameters are very close to those of $ZrTiO_4$ crystal (JCPDS file No. 74-1504). No XRD peaks corresponding to TiO_2 and ZrO_2 phases can be detected in XRD patterns of samples calcined in the range of 350 - 1200 °C. The previous studies [12, 13] showed that the direct crystallization of $ZrTiO_4$ at low temperature (<600 °C) is due to the high level of homogeneity of the xerogel. In the case of low homogeneity, TiO_2 crystallization occurs before the crystallization of $ZrTiO_4$ phase.

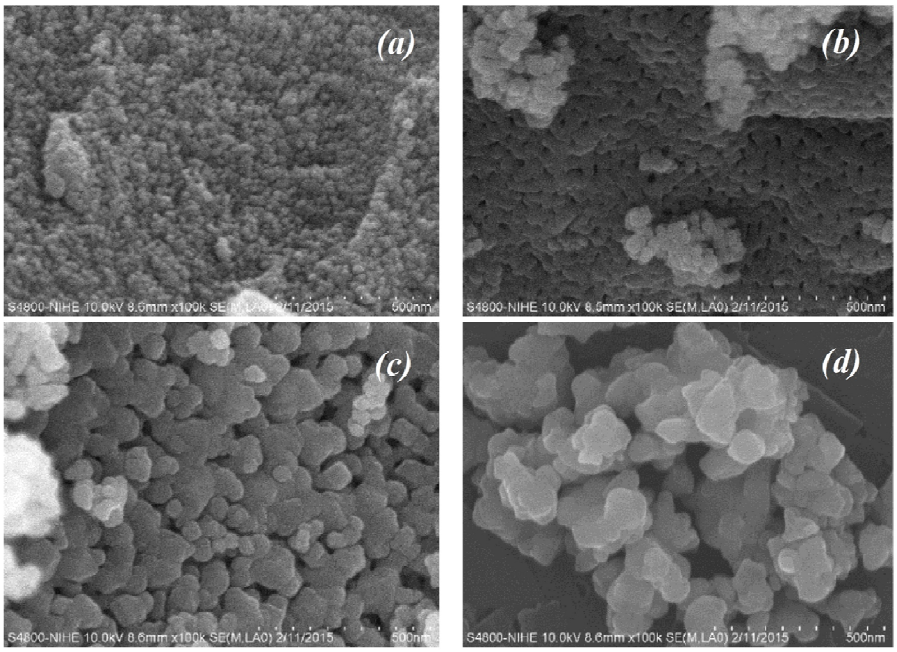

Figure 2. FE-SEM images of $ZrTiO_4$ samples: (a) ZT450, (b) ZT800, (c) ZT1000 and (d) ZT1200.

The influence of calcining temperature on particle size of $ZrTiO_4$ can be observed in Fig. 2. As depicted in Fig. 2a, despite being in amorphous phase, ZT450 sample existed in nanoparticles of about 10 nm in size with relatively spherical shape and no agglomeration. This small grain size is believed to have a large surface area that is suitable for an efficient photocatalytic performance, besides many other factors are required. The FE-SEM images exhibit increasing in particle size with the increase of calcining temperature, gradually to about of 20, 50 and 100 nm for ZT800, ZT1000 and ZT1200 samples, respectively. This shows that the calcining temperature was strongly affected to crystalline growth of the samples. The FE-SEM image of ZT800 sample shows a high homogeneous particle size. When the calcining temperature continuously increases, the particles become much larger and different in size. In the SEM of ZT1200 sample (with a high calcining temperature), the particle boundaries are not clearly observed. With suitable crystallinity, small particle size and the uniform of morphology, ZT800 sample can be considered as the most promising sample for the efficient photocatalytic performance.

To assess the energy band structure evolution in the course of heating, the UV-Vis absorption spectra were conducted on amorphous and crystalline samples, as presented in Fig. 3a. The absorption spectrum of ZT450 sample exhibits a tail in the wavelength region of 400 - 600 nm, beside an exponential optical edge. The nature of these behaviors was assigned to the existence of defect states in the band gap [14, 15] which are promoted by the disorder structure of amorphous phase. The presence of $Ti(Zr)O_5$ groups in $ZrTiO_4$ amorphous phase can create the new energy states which locate

in the energy gap, similarly to Longo's report [15] on amorphous $Ba_{0.5}Sr_{0.5}TiO_3$. The values of the optical band gap corresponding to different calcining temperatures were calculated using Wood and Tauc plot [16] and displayed in Fig. 3b. The increase of the optical band gap indicates the narrowing of allowed energy bands with the increase of calcining temperature. The value of optical band gap is about of 3.34, 3.37, and 3.46 eV for samples ZT450, ZT800, and ZT1000, respectively.

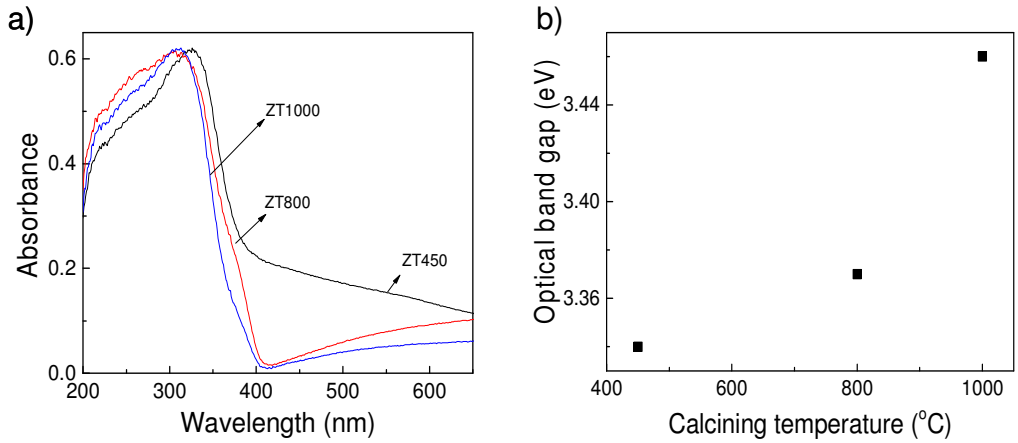

Figure 3. a) Absorption spectra of $ZrTiO_4$ samples and b) the dependence of optical band gap E_g on calcining temperature.

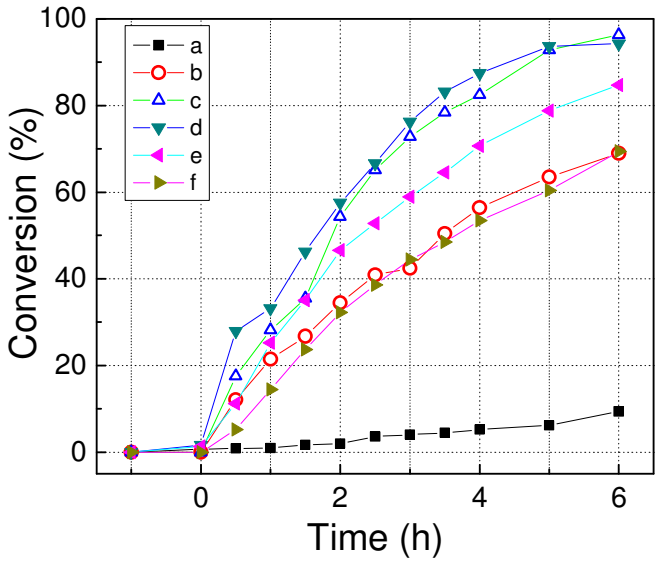

Figure 4. Conversion values for RhB (10 ppm): (a) adsorption process in dark using ZT450 sample and photodegradation under Xenon light (300W) using (b) ZT450, (c) ZT700, (d) ZT800, (e) ZT1000, and (f) ZT1200 samples.

Photocatalytic performance of amorphous and crystaline $ZrTiO_4$ samples was carried out through the photodegradation of RhB under the Xenon lamp irradiation which partly contains the UV light. In Fig. 4, curve (a) presents the conversion percentage of RhB in ZT450 powder solution without irradiation. The efficiency of the photocatalytic performance increases in the first range of calcining temperature from 450 to 800 °C, reaches a largest value for ZT800 sample, and gradually decreases for the sample calcined at higher temperatures. Despite being in amorphous phase with the strong distorted structure, ZT450 sample exhibits a large photocatalytic efficiency, namely about 70 % RhB conversion under 6 hours irradiation. This value is the same with that of ZT1200 sample. This behavior indicates that the efficient photocatalytic performance is dependent on both the particle size and the crystallinities of the samples. The largest efficiency of the photocatalytic performance obtained for the ZT800 sample can be assigned to both their small and homogeneous particle size and the suitable low crystallinities. The larger particle size of the samples calcined at higher temperatures leads to the decrease of the effective surface area, consequently lowering the photocatalytic efficiency.

4. Conclusion

The onset of the crystallization of $ZrTiO_4$ from xerogel was found to be nearly 600 °C as observed by XRD patterns. FE-SEM micrographs showed that $ZrTiO_4$ samples have relatively spherical particle shape with the increase of the particle size as the calcining temperature increases. The largest efficiency of photocatalytic performance was found out through RhB degradation under irradiation of Xenon lamp for a suitable low crystallinity in $ZrTiO_4$ powder calcined at 800 °C.

Acknowledgments

This research is funded by Vietnam National Foundation for Science and Technology Development (NAFOSTED) under grant number 103.02-2014.21.

References

[1] Kim, Y.-J., et al., Influence of the Microstructures on the Dielectric Properties of $ZrTiO_4$ Thin Films at Microwave-Frequency Range. Jpn. J. Appl. Phys., 2001. 40: p. 4599-4603.

[2] Liu, S.-W., et al., Preparation and photocatalytic activities of $ZrTiO_4$ nanocrystals. J. Alloys Compd., 2007. 437: p. L1-L3.

[3] Salahinejad, E., et al., Surface Modification of Stainless Steel Orthopedic Implants Sol-Gel $ZrTiO_4$ and $ZrTiO_4$-PMMA Coatings. J. Biomed. Nanotechno., 2013. 9: p. 1327-1335.

[4] Chang, D.A., P. Lin, and T.Y. Tsenga, Growth of highly oriented ZrTi04 thin films by radio-frequency sputtering. Appl. Phys. Lett., 1994. 64(24): p. 3252-3254.

[5] Yu, J.C., et al., $Ti_{1-x}Zr_xO_2$ Solid Solutions for the Photocatalytic Degradation of Acetone in Air. J. Phys. Chem. B, 1998. 102: p. 5094-5098.

[6] Marfunin, S., Physics of Minerals and Inorganic Materials. 1979, New York: Springer Berlin Heidelberg.

[7] Burns, R.G., Mineralogical applications of crystal field theory. 1993, Cambridge University Press.

[8] Mao, C.-B., L.-A. Zhou, and X.-Y. Sun, Optimization of the solution-sol-gel process to synthesize homogeneous BiPbSrCaCuO powder. Phys. C, 1997. 281: p. 27-34.

[9] Balamurugan, A., S. Kannan, and S. Rajeswari, Structural and electrochemical behaviour of sol-gel zirconia films on 316L stainless-steel in simulated body fluid environment. Mater. Lett., 2003. 57: p. 4202–4205.

[10] Ehrhart, G., et al., Structural and optical properties of n-propoxide sol–gel derived ZrO_2 thin films. Thin. Solid Films, 2006. 496: p. 227-233.

[11] Vittayakorn, N., Synthesis and a crystal structural study of microwave dielectric Zirconium Titanate ($ZrTiO_4$) powders via a mixed oxide synthesis route. J. Ceram. Proc. Res., 2006. 7(4): p. 288-291.

[12] Navio, J.A., et al., Formation of zirconium titanate powder from a sol-gel prepared reactive precursor. J. Mater. Sci., 1992. 27: p. 2463-2467.

[13] Salahinejad, E., et al., Aqueous sol–gel synthesis of zirconium titanate ($ZrTiO_4$) nanoparticles using chloride precursors. Ceram. Inter., 2012. 38: p. 6145-6149.

[14] Yamasaki, S., et al., Annealing studies on low optical absorption of gd a-Si:H using photoacoustic spectroscopy. J. Phys., 1981. 42: p. 297-300.

[15] Longo, E., et al., Density functional theory calculation of the electronic structure of $Ba_{0.5}Sr_{0.5}TiO_3$: Photoluminescent properties and structural disorder. Phys. Rev. B 2004. 69: p. 125115.

[16] Wood, D.L. and J. Tauc, Weak Absorption Tails in Amorphous Semiconductors. Phys. Rev. B, 1972. 5: p. 3144.